IET Communications

Research Article

IET Journals
The Institution of Engineering and Technology

Coordinated multicell beamforming for massive multiple-input multiple-output systems based on uplink–downlink duality

ISSN 1751-8628
Received on 7th November 2015
Revised on 26th June 2016
Accepted on 30th July 2016
doi: 10.1049/iet-com.2015.1045
www.ietdl.org

Shiwen He ✉, *Yongming Huang, Yanru Shi, Chenhao Qi, Shi Jin, Luxi Yang*

School of Information Science and Engineering, Southeast University, Nanjing 210096, People's Republic of China
✉ *E-mail: shiwenhe@seu.edu.cn*

Abstract: This paper studies joint beamforming and power allocation for multicell multiuser multi-antenna systems with the objective of maximising the minimum signal-to-interference-plus-noise ratio (max–min SINR). The authors first consider developing an iterative algorithm to achieve the optimal performance by extending the uplink–downlink duality for finite-scale wireless communication systems. The solution is then generalised to achieve the asymptotically optimal multicell beamforming with the aim to reduce the overhead of signalling exchange between coordinated base stations based on large dimension random matrix theory. Based on that, an efficient multicell beamforming algorithm is proposed to asymptotically achieve the max–min SINR. To further solve the complexity issue of large dimensional matrix inversion involved in the calculation of beamforming vectors, they propose a low-complexity beamforming calculator based on truncated polynomial expansion approach. Numerical results validate the effectiveness of the authors' proposed algorithms and show that they can achieve the optimal or asymptotically optimal performance in a massive multi-input multi-output system with low complexity and small backhaul overhead.

1 Introduction

To meet the demands for explosive increase of data traffic and the number of user terminals, massive multiple-input multiple-output (MIMO) technology has emerged as a promising solution and has attracted a lot of research interest [1], due to its potential of significantly improving performance in terms of both data rate and link reliability. Owing to the increased number of base station (BS) antennas, exceptional array gain and high spatial resolution can be obtained for the massive MIMO systems [1–4]. In particular, it was revealed that a simple linear precoding with a large enough transmit antenna array is able to completely mitigate the effect of the inter-user interference and noise, provided that channel state information (CSI) of users is ideally available at the BS. The major hurdle is that acquiring CSI will cause too much training overhead in a frequency division duplexing system and may suffer pilot contamination problem in a time division duplexing system.

Note that the inter-cell interference (ICI) is being the major problem which affects the system performance especially regarding the cell-edge users for cellular communication systems. In order to reduce the ICI, coordinated multi-point transmission and reception technology has been intensively studied [5–8]. Among them, the uplink–downlink duality theory has been a key technology which can be exploited to solve the optimisation problem of joint beamforming and power allocation [9, 10]. The key idea is that the original downlink problem with coupling beamformers can be recast as a virtual uplink problem that has the closed-form structure of the optimal beamformers. To leverage the uplink–downlink duality, the signal-to-interference plus-noise ratio (SINR) balancing problem was first addressed using the extended coupling matrix [9]. However, it is only subjected to a single sum-power constraint. Later, the uplink–downlink duality theory was extended to the case of per-BS power constraints and was then exploited to efficiently tackle the max–min SINR problem [10].

Recently, the design of coordinated multicell downlink beamforming of multicell massive MIMO communication systems was studied by jointly using the uplink–downlink duality and random matrix theory [11, 12]. Motivated by the fact that the deterministic approximation of achievable SINR or rate in massive MIMO system approaches the true value when the system dimension tends to infinity [13–16], an asymptotic uplink–downlink duality was proposed. Based on that, an efficient coordinated beamforming algorithm was proposed for massive MIMO systems, in which the beamforming vectors at each BS were readily obtained only using local CSI while the power allocation was calculated only using the large-scale fading factors of channels. It was disclosed that most gain of coordinated beamforming in multicell massive MIMO system can be obtained only using partial CSI. The authors of [11] investigated the max–min SINR problem by jointly using the bisection method and solving the problem of the power minimisation of dual virtual uplink problem for massive MIMO communication systems. Huang *et al.* studied the max-min SINR problem via combining the fixed-point equation theory [17, 18] and the uplink–downlink duality for multicell massive MIMO communication systems subject to a total power constraint [12]. Bannour *et al.* investigated the duality between the number of antennas in MIMO and the number of subcarriers in orthogonal frequency division multiplexing (OFDM) and illustrated that a negligible gap between massive MIMO-OFDM and conventional MIMO-OFDM with a large number of subcarriers in [19]. The tradeoff of the energy and spectral efficiency was investigated for the uplink of large-scale multiuser MIMO system with fixed receivers, such as zero-forcing, maximum ratio combining, and minimum mean square errors (MMSE) receiver. It has been shown that the use of moderately large antenna arrays can improve the spectral and energy efficiency with orders of magnitude compared with the single-antenna system [20]. To improve the efficiency of RF power amplifiers, Mohammed and Larsson investigated the design of the constant envelope precoding for large-scale multiuser MIMO system [21]. However, the max–min SINR problem for multicell massive MIMO systems subject to a per-BS power constraint is not investigated from the perspective of the fixed-point theory and the uplink–downlink duality based on statistical CSI.

In this paper, we study coordinated joint beamforming and power allocation by using the fixed-point equation theory [17, 18] and the uplink–downlink duality for multicell multiuser multiple-input single-output (MISO) downlink systems subject to per-BS power constraints. In particular, our goal is to find a distributed solution by jointly utilising the long-term and short-term CSI, so as to exploit the potential gain of multicell multiuser MISO channels with limited overhead for acquiring CSI and backhaul. Different from the problem considered in [12], the problem of interest is to maximise the minimum SINR subject to per-BS power constraints, where a general spatially correlated MISO channel model is considered. The main contributions are listed below:

- By extending the uplink–downlink duality, the max–min SINR multicell beamforming with per-BS power constraints is transformed into an equivalent and more tractable virtual uplink form for finite-scale system. Then, an iterative algorithm with guaranteed convergence is presented to solve the virtual uplink problem, by which the optimal beamforming and power allocation are achieved by converting the virtual uplink solution to the downlink.
- The above idea is generalised to achieve the asymptotically optimal multicell beamforming for massive MIMO system. In particular, by exploiting the hardening effect of massive MIMO channels, we use the derived deterministic equivalentence of achievable SINR as the objective and generalise the uplink–downlink duality into a large-scale regime where the solution conversion from the uplink to the downlink only needs statistical CSI. Then, an efficient multicell beamforming solution is proposed to asymptotically achieve the max–min SINR, in which the power allocation is calculated on a long-term basis while the beamforming vector is obtained with a closed-form expression on a short-term basis. Our analysis shows that the proposed solution asymptotically achieves the optimal performance as the number of transmit antennas tends to infinity, but with much reduced backhaul overhead and computational complexity.
- To further address the issue of large dimensional matrix inversion involved in the calculation of beamforming vectors, a low-complexity beamforming calculator is presented based on truncated polynomial expansion (TPE) approach. In particular, in order to guarantee the performance of such a low-complexity solution, we derive the equivalent form of the uplink SINR achieved by the TPE beamforming. Then, a new optimisation problem is formulated and solved to calculate the polynomial coefficients of TPE beamforming which only requires the statistical CSI. Numerical results show that the TPE based beamforming is effective even with a very small value of truncating order, thus with significantly reduced computational complexity.

The remaining of this paper is organised as follows. The system model is described in Section 2. In Section 3, a coordinated multicell beamforming algorithm is proposed for finite-scale system. Then, a coordinated multicell beamforming algorithm is proposed for large-scale system in Section 4. In Section 5, a lower complexity algorithm is proposed to reduce the computational complexity. The simulation results are shown in Section 6 and conclusions are finally given in Section 7.

The following notations are used throughout this paper. Bold lowercase and uppercase letters represent column vectors and matrices, respectively. The superscripts $^{\mathrm{T}}$, $^{\mathrm{H}}$ and † represent the transpose operator, conjugate transpose operator, the Moore Penrose pseudo-inverse of matrix, respectively. $\|\cdot\|$ denotes the Euclidean norm for vector or the Frobenius norm for matrix. $\lceil\cdot\rceil$ and $\lfloor\cdot\rfloor$ denote the ceiling function and the floor function, respectively.

2 System model

Consider a K-cell multiuser-MISO downlink transmission system where the jth BS is equipped with M_j transmit antennas and serves I single-antenna users in cell j, $j = 1, \dots, K$. We denote the kth user in cell j as user-(j, k) and BS in cell m as BS-m. The received signal $y_{j,k}$ for user-(j, k) is written as

$$y_{j,k} = \sum_{m=1}^{K}\sum_{n=1}^{I}\sqrt{p_{m,n}}\boldsymbol{h}_{m,j,k}^{\mathrm{H}}\boldsymbol{w}_{m,n}x_{m,n} + n_{j,k}, \tag{1}$$

where $p_{j,k}$ represents the transmit power for user-(j, k), $\boldsymbol{h}_{m,j,k}$ denotes the flat fading channel vector from the mth BS to user-(j, k), $\boldsymbol{w}_{j,k}$ denotes the normalised beamforming vector for user-(j, k) ($\|\boldsymbol{w}_{j,k}\| = 1$), $x_{j,k}$ is the information signal intended for user-(j, k), and $n_{j,k}$ is a zero-mean circularly symmetric complex Gaussian random noise with variance $\sigma_{j,k}^2$. Further, the channel vector $\boldsymbol{h}_{m,j,k}$ is modelled as

$$\boldsymbol{h}_{m,j,k} = \boldsymbol{\Phi}_{m,j,k}^{1/2}\boldsymbol{z}_{m,j,k}, \tag{2}$$

where

$$\boldsymbol{\Phi}_{m,j,k} \sim \mathcal{CN}\left(0, \frac{d_{m,j,k}\boldsymbol{R}_{m,j,k}}{M_j}\right),$$
$$\boldsymbol{z}_{m,j,k} \sim \mathcal{CN}\left(0, \boldsymbol{I}_{M_j}\right),$$

denotes the large-scale channel effect, and the channel covariance matrix $\boldsymbol{R}_{m,j,k} \in \mathbb{C}^{M_j\times M_j}$ satisfies the following conditions

$$\lim\ \sup\left\|\boldsymbol{R}_{m,j,k}\right\| < +\infty, \quad \forall m, j, k, \tag{3}$$

$$\lim\ \inf\frac{1}{M_j}\mathrm{tr}\left(\boldsymbol{R}_{m,j,k}\right) > 0, \quad \forall m, j, k. \tag{4}$$

For description convenience, the K-cell MU-MISO downlink transmission system formulated in (1) is modelled as an interference network with $\bar{I} = KI$ users, by which user-$(\lceil m/I\rceil, m - I\lfloor m/I\rfloor)$ can be simply denoted as user-m, $m = 1, \dots, \bar{I}$. For simplicity, let $\boldsymbol{h}_{n,m} = \boldsymbol{h}_{\lceil n/I\rceil,\lceil m/I\rceil,m-I\lfloor m/I\rfloor}$, $p_m = p_{\lceil m/I\rceil,m-I\lfloor m/I\rfloor}$, $\boldsymbol{w}_m = \boldsymbol{w}_{\lceil m/I\rceil,m-I\lfloor m/I\rfloor}$, $\boldsymbol{\gamma}_m = \boldsymbol{\gamma}_{\lceil m/I\rceil,m-I\lfloor m/I\rfloor}$, and $\sigma_m^2 = \sigma^2_{\lceil m/I\rceil,m-I\lfloor m/I\rfloor}$ denote, respectively, the channel coefficient between the BS-n and the user-m, the transmit power, the normalised beamforming vector, the SINR, and the noise variance for user-m. The achievable SINR of user-m is calculated as

$$\boldsymbol{\gamma}_m = \frac{p_m\left\|\bar{\boldsymbol{h}}_{m,m}^{\mathrm{H}}\boldsymbol{w}_m\right\|^2}{\sum_{n\neq m} p_n\left\|\bar{\boldsymbol{h}}_{n,m}^{\mathrm{H}}\boldsymbol{w}_n,\right\|^2 + 1} \tag{5}$$

where $\bar{\boldsymbol{h}}_{n,m} = (\boldsymbol{h}_{n,m}/\sigma_m)$. To achieve the fairness among the users, we focus on the max–min SINR optimisation problem given as

$$\begin{cases} \max\limits_{\{\boldsymbol{w}_m, p_m\}}\ \min\limits_{m} \boldsymbol{\gamma}_m \\ \text{s.t.} \sum\limits_{m=(j-1)I+1}^{jI} p_m \le P_j, p_m \ge 0, \|\boldsymbol{w}_m\| = 1. \end{cases} \tag{6}$$

where P_j is the maximum allowable transmit power of the jth BS.

3 Algorithm for finite-scale system

Due to the coupling of the optimisation variables, it is seen that the problem (6) is non-convex and thus difficult to solve directly. In order to decouple the optimisation variables, in this section, we resort to transforming the downlink problem into the dual virtual uplink optimisation problem by extending the uplink–downlink duality and obtain the solution of original problem by combining the fixed-point equation theory. To proceed, we introduce some auxiliary variables $\{v_j\}_{j=1}^{K}$ which represent the virtual noise variance. Then the problem (6) with intractable per-BS power constraints is transformed as follows

$$\begin{cases} \min\limits_{v_j} \max\limits_{\{\boldsymbol{w}_m, p_m\}} \min\limits_{m} \boldsymbol{\gamma}_m \\ \text{s.t.} \sum\limits_{m=1}^{\bar{I}} v_{\lceil m/I \rceil} p_m \le \sum\limits_{j=1}^{K} v_j P_j,\ p_m \ge 0,\ \|\boldsymbol{w}_m\| = 1 \end{cases} \tag{7}$$

The existing results in [9–12] have revealed that the problem (7) is dual to the following problem

$$\begin{cases} \min\limits_{v_j} \max\limits_{\{\boldsymbol{w}_m, \lambda_m\}} \min\limits_{m} \boldsymbol{\gamma}_m \\ \text{s.t.} \sum\limits_{m=1}^{\bar{I}} \lambda_m \le \sum\limits_{j=1}^{K} v_j P_j,\ \lambda_m \ge 0,\ \|\boldsymbol{w}_m\| = 1. \end{cases} \tag{8}$$

where λ_m denotes the transmit power of the virtual uplink user-m, and $\boldsymbol{\gamma}_m$ is the virtual uplink SINR for user-m and is given by

$$\boldsymbol{\gamma}_m = \frac{\lambda_m \left\| \bar{\boldsymbol{h}}_{m,m}^{\mathrm{H}} \boldsymbol{w}_m \right\|^2}{\sum_{n=1, n \ne m}^{\bar{I}} \lambda_n \left\| \bar{\boldsymbol{h}}_{m,n}^{\mathrm{H}} \boldsymbol{w}_m \right\|^2 + v_{\lceil m/I \rceil}}. \tag{9}$$

It is easy to see that the optimisation problem (8) is convex in $\{v_j\}$, the problem (7) with respect to variables $\{v_j\}$ can be solved via a subgradient projection method, and the subgradient of $\{v_j\}$ is given by $\boldsymbol{g} = \left[P_1 - \sum_{k=1}^{I} p_{1,k},\ \ldots,\ P_K - \sum_{k=1}^{I} p_{K,k}\right]$. Fixing $\{\lambda_n\}$ and $\{v_j\}$, the optimal receive beamformer is the MMSE receiver which has an analytic structure, given by

$$\boldsymbol{w}_m^{\mathrm{opt}} = \frac{\left(\sum_{n \ne m} \lambda_n \bar{\boldsymbol{h}}_{m,n} \bar{\boldsymbol{h}}_{m,n}^{\mathrm{H}} + v_{\lceil m/I \rceil} \boldsymbol{I}_{M_{\lceil m/I \rceil}}\right)^{-1} \bar{\boldsymbol{h}}_{m,m}}{\left\| \left(\sum_{n \ne m} \lambda_n \bar{\boldsymbol{h}}_{m,n} \bar{\boldsymbol{h}}_{m,n}^{\mathrm{H}} + v_{\lceil m/I \rceil} \boldsymbol{I}_{M_{\lceil m/I \rceil}}\right)^{-1} \bar{\boldsymbol{h}}_{m,m} \right\|}. \tag{10}$$

According to the results obtained in [12], the uplink transmit power with given $\boldsymbol{\gamma}_m$ can be iteratively updated as follows

$$\lambda_m = \boldsymbol{\gamma}_m \frac{\left(\sum_{n=1, n \ne m}^{\bar{I}} \lambda_n \left\| \bar{\boldsymbol{h}}_{m,n}^{\mathrm{H}} \boldsymbol{w}_m \right\|^2 + v_{\lceil m/I \rceil}\right)}{\left\| \bar{\boldsymbol{h}}_{m,m}^{\mathrm{H}} \boldsymbol{w}_m \right\|^2}, \quad \forall m. \tag{11}$$

Once the dual uplink problem (8) has been solved, according to the uplink–downlink duality theory, the optimal uplink beamforming vectors are the beamforming solution of the original downlink problem, while the power solution of the downlink problem can also be obtained from the uplink power allocation. Defining an extended power vector $\tilde{\boldsymbol{p}} = \begin{bmatrix} \boldsymbol{p} \\ 1 \end{bmatrix}$, and an extended coupling matrix

$$\boldsymbol{Q} = \begin{bmatrix} \boldsymbol{DG} & \boldsymbol{D}\boldsymbol{1}_{\bar{I}} \\ \dfrac{1}{P_{\max}} \tilde{\boldsymbol{v}}^{\mathrm{T}} \boldsymbol{DG} & \dfrac{1}{P_{\max}} \tilde{\boldsymbol{v}}^{\mathrm{T}} \boldsymbol{D}\boldsymbol{1}_{\bar{I}}, \end{bmatrix} \tag{12}$$

where $P_{\max} = \sum_{j=1}^{K} v_j P_j$, the matrices $\boldsymbol{G}$ and $\boldsymbol{D}$ are, respectively, given by

$$\boldsymbol{G}_{m,n} = \begin{cases} 0 & m = n \\ \left\| \bar{\boldsymbol{h}}_{n,m}^{\mathrm{H}} \boldsymbol{w}_n \right\|^2, & m \ne n, \end{cases} \tag{13}$$

$$\boldsymbol{D}_{m,n} = \left\{ \frac{\boldsymbol{\gamma}_m}{\left\| \bar{\boldsymbol{h}}_{m,m}^{\mathrm{H}} \boldsymbol{w}_m \right\|^2},\ m = n,\ 0,\ m \ne n, \right. . \tag{14}$$

and $\tilde{\boldsymbol{v}} = \Big(\underbrace{v_1 \cdots v_1}_{I} \underbrace{v_2 \cdots v_2}_{I} \cdots \underbrace{v_K \cdots v_K}_{I}\Big)^{\mathrm{T}}$. The conclusions in [9] have revealed that the optimal power vector $\boldsymbol{p}$ is obtained as the first $\bar{I}$ components of the dominant eigenvector of $\boldsymbol{Q}$, which can be scaled so that its last component equals one.

In summary, the distributed algorithm computing the optimal solution of the problem (7) is given in Algorithm 1 (Fig. 1) where $\boldsymbol{f}_{\max}$ is the maximum eigenvector of the extended coupling matrix of $\boldsymbol{Q}$, ς is the update step-size, $\boldsymbol{g}$ is the subgradient of the virtual noise vector $\boldsymbol{v}$, ε denotes the threshold of inner iteration, and δ denotes the threshold of outer iteration. It is easy to see that the main computational complexity in Algorithm 1 (Fig. 1) is the matrix inversion and the singular value decomposition (SVD) in steps 4 and 6. The complexity of the matrix inversion and the SVD of $M \times M$ matrix is $\mathcal{O}(M^{2.736})$ and $\mathcal{O}(M^3)$, respectively [22]. Therefore, in Algorithm 1 (Fig. 1), the complexity of the matrix inversion is $\phi \sum_{j=1}^{K} \mathcal{O}\left(M_j^{2.736}\right)$ and the complexity of the SVD is $\varphi \mathcal{O}\left((KI+1)^3\right)$, where ϕ and φ denote, respectively, the number of the iterations of steps 4 and 6.

4 Algorithm for large-scale system

The beamforming vectors can be efficiently calculated via analytical expression, however, the iterative update of both the beamformers and the power allocation is based on the instantaneous CSI in Algorithm 1 (Fig. 1) designed for finite-scale system. The

Algorithm 1

1: Initialise $\mathbf{v}[0] \in R_+^{\bar{I}}$, $i = 0$;

2: Initialise $\boldsymbol{\lambda}[0] \in R_+^{\bar{I}}$, $\mathbf{w}_m[0] \in \mathbb{C}^{M_j \times \bar{I}} \forall m$ such that $\sum\limits_{\mathrm{m}=1}^{\bar{I}} \lambda_m[0] \le \sum\limits_{j=1}^{K} v_j[i] P_j$, $\|\mathbf{w}_m[0]\| = 1$, $l = 0$;

3: Let $l = l + 1$, compute $\boldsymbol{\gamma}_m$ with $\mathbf{v}[i], \lambda[l-1]$, and $\mathbf{w}_m[l-1]$, then update the uplink power $\boldsymbol{\lambda}[l]$:

$$\lambda_m[l] = \frac{1}{\boldsymbol{\gamma}_m} \lambda_m[l-1]\ , \quad \forall m,$$

and normalise $\boldsymbol{\lambda}[l]$ as

$$\boldsymbol{\lambda}[l] \leftarrow \frac{\sum\limits_{j=1}^{K} v_j[i] P_j}{\sum\limits_{\mathrm{m}=1}^{\bar{I}} \lambda_m[l]} \boldsymbol{\lambda}[l].$$

4: Update the transmit beamformer $\mathbf{w}_m[l]$ with $\mathbf{v}[i]$, $\lambda[l]$ and (10);

5: If $|\boldsymbol{\lambda}[l] - \boldsymbol{\lambda}[l-1]| > \varepsilon$, return to step 3; otherwise, go to step 6;

6: According to (13), (14), (12), compute $\mathbf{G}_{m,n}$, $\mathbf{D}_{m,n}$ and $\mathbf{Q}$; then update downlink power $\mathbf{p}$, i.e. $\mathbf{p} = \left[\mathbf{f}_{\max} / (\mathbf{f}_{\max})_{\bar{I}+1}\right]_{1 \sim \bar{I}}$;

7: Let $i = i + 1$, update $\mathbf{v}[i]$ with subgradient method, if $\|\mathbf{v}[i] - \mathbf{v}[i-1]\| > \delta$, return to step (2); otherwise, the iteration stops.

Fig. 1 *Multicell MU-MISO max–min SINR optimisation*

IET Commun., 2016, Vol. 10, Iss. 17, pp. 2380–2390

overhead of the signalling exchange between coordinated BSs is mainly determined by the update frequency of the transmit power allocation. In what follows, we try to reduce the overhead of the signalling exchange between the coordinated BSs by exploiting the large-scale random matrix theory. In other words, if the power $\boldsymbol{p}$ and $\boldsymbol{\lambda}$ in the communication system converge to some deterministic values that only rely on statistical channel information, then these deterministic values can be a priori calculated, stored, and updated only when the channel statistics change. Thereafter, the beamforming vector can be computed using these slowly updated power values and the available instantaneous local CSI. To proceed, we assume that both the number of transmit antennas M_j and the number of users per cell I go to infinity while their ratio $\lim(I/M_j)$, $\forall j$ remains bounded.

Plugging the MMSE beamforming (10) in the expression of the uplink SINR (9) of user-$(\lceil m/I \rceil, m - I\lfloor m/I \rfloor)$, we have

$$\boldsymbol{\gamma}_m = \lambda_m \bar{\boldsymbol{h}}_{m,m}^{\mathrm{H}} \left(\sum_{n \neq m} \lambda_n \bar{\boldsymbol{h}}_{m,n} \bar{\boldsymbol{h}}_{m,n}^{\mathrm{H}} + v_{\lceil m/I \rceil} \boldsymbol{I}_{M_{\lceil m/I \rceil}} \right)^{-1} \bar{\boldsymbol{h}}_{m,m}. \tag{15}$$

Though the instantaneous SINR in (15) is a random variable in quadratic form for each random instantaneous CSI, its asymptotic approximation only depends on the empirical distribution of the eigenvalues for $\left(\sum_{n \neq m} \lambda_n \bar{\boldsymbol{h}}_{m,n} \bar{\boldsymbol{h}}_{m,n}^{\mathrm{H}} + v_{\lceil m/I \rceil} \boldsymbol{I}_{M_{\lceil m/I \rceil}} \right)^{-1}$, given by the following Lemma 1.

Lemma 1: The instantaneous SINR $\boldsymbol{\gamma}_m$ can be approximated by a deterministic quality $\boldsymbol{Y}_m$ such that $\boldsymbol{Y}_m - \boldsymbol{\gamma}_m \xrightarrow[M_{\lceil m/I \rceil} \to \infty]{\text{a.s.}} 0$ as the system dimension $M_{\lceil m/I \rceil} \to \infty$. $\boldsymbol{Y}_m$ is given by

$$\boldsymbol{Y}_m = \lambda_m \mathrm{tr} \left(\bar{\boldsymbol{\Phi}}_{m,m} \left(\sum_{n \neq m} \lambda_n \bar{\boldsymbol{h}}_{m,n} \bar{\boldsymbol{h}}_{m,n}^{\mathrm{H}} + v_{\lceil m/I \rceil} \boldsymbol{I}_{M_{\lceil m/I \rceil}} \right)^{-1} \right). \tag{16}$$

Also, $\boldsymbol{Y}_m$ is described by the following fixed-point equation

$$\boldsymbol{Y}_m = \lambda_m \frac{1}{\bar{I}} \mathrm{tr}\left(\bar{\boldsymbol{\Phi}}_{m,m} \boldsymbol{T}_m \right), \quad \forall m, \tag{17}$$

where

$$\begin{aligned}
\bar{\boldsymbol{\Phi}}_{m,m} &= \frac{\boldsymbol{\Phi}_{m,m}}{\sigma_m^2} = \frac{d_{m,m}}{\sigma_m^2 M_{\lceil m/I \rceil}} \boldsymbol{R}_{m,m}, \\
\bar{\boldsymbol{\Phi}}_{m,n} &= \frac{\boldsymbol{\Phi}_{m,n}}{\sigma_n^2} = \frac{d_{m,n}}{\sigma_n^2 M_{\lceil m/I \rceil}} \boldsymbol{R}_{m,n}, \\
\boldsymbol{T}_m &= \left(\frac{\lambda_n}{\bar{I}} \sum_{n=1, n \neq m}^{\bar{I}} \frac{d_{m,n} \boldsymbol{R}_{m,n}}{M_{\lceil m/I \rceil} \sigma_n^2} \frac{1}{1 + \delta_n} + \frac{1}{\bar{I}} v_{\lceil m/I \rceil} \boldsymbol{I}_{M_{\lceil m/I \rceil}} \right)^{-1}, \\
\delta_n &= \frac{1}{\bar{I}} \mathrm{tr}\left(\lambda_n \bar{\boldsymbol{\Phi}}_{m,n} \boldsymbol{T}_m \right).
\end{aligned}$$

Proof: According to Lemmas 3 and 4 given in the Appendix, we have

$$\begin{aligned}
\boldsymbol{\gamma}_m &= \lambda_m \bar{\boldsymbol{h}}_{m,m}^{\mathrm{H}} \left(\sum_{n \neq m} \lambda_n \bar{\boldsymbol{h}}_{m,n} \bar{\boldsymbol{h}}_{m,n}^{\mathrm{H}} + v_{\lceil m/I \rceil} \boldsymbol{I}_{M_{\lceil m/I \rceil}} \right)^{-1} \bar{\boldsymbol{h}}_{m,m} \\
&\xrightarrow[M_{\lceil m/I \rceil} \to \infty]{\text{a.s.}} \lambda_m \frac{1}{\bar{I}} \mathrm{tr}\left(\bar{\boldsymbol{\Phi}}_{m,m} \boldsymbol{T}_m \right).
\end{aligned} \tag{18}$$

□

Based on the existing results in [9–12], once the optimal solution of the max–min SINR optimisation problem is obtained, all users achieve the same optimal balanced SINR. Thus, the virtual uplink transmit power can be updated by

$$\lambda_m = \frac{\boldsymbol{Y}_m}{(1/\bar{I}) \mathrm{tr}\left(\bar{\boldsymbol{\Phi}}_{m,m} \boldsymbol{T}_m \right)}, \quad \forall m, \tag{19}$$

and the virtual uplink transmit power must satisfy $\sum_{m=1}^{\bar{I}} \lambda_m \leq \sum_{j=1}^{K} v_j P_j$, then both the downlink transmit power and the virtual noise variance can be obtained. Similarly, the instantaneous random variable $\boldsymbol{\gamma}_m$ can be applied to obtain the asymptotic approximation of the elements of $\tilde{\boldsymbol{G}}$ and $\tilde{\boldsymbol{D}}$ are described as the following Theorem 1.

Theorem 1: The elements of the instantaneous extended coupling matrices $\boldsymbol{G}$ and $\boldsymbol{D}$ can be approximated as $\tilde{\boldsymbol{G}}_{m,n} - \boldsymbol{G}_{m,n} \xrightarrow[M_{\lceil m/I \rceil} \to \infty]{\text{a.s.}} 0$ and $\tilde{\boldsymbol{D}}_{m,n} - \boldsymbol{D}_{m,n} \xrightarrow[M_{\lceil m/I \rceil} \to \infty]{\text{a.s.}} 0$, respectively, as the system dimension $M_{\lceil m/I \rceil} \to \infty$, where

$$\tilde{\boldsymbol{G}}_{m,n} = \begin{cases} 0, & m = n, \\ \dfrac{(1/\bar{I}) \mathrm{tr}\left(\bar{\boldsymbol{\Phi}}_{n,n} \boldsymbol{T}_n \bar{\boldsymbol{\Phi}}_{n,m} \boldsymbol{T}_n \right)}{\mathrm{tr}\left(\bar{\boldsymbol{\Phi}}_{n,n} \boldsymbol{T}'_n \right) \left(1 + \lambda_m (1/\bar{I}) \mathrm{tr}\left(\bar{\boldsymbol{\Phi}}_{n,m} \boldsymbol{T}_n \right) \right)^2}, & m \neq n, \end{cases} \tag{20}$$

$$\tilde{\boldsymbol{D}}_{m,n} = \begin{cases} \dfrac{\boldsymbol{Y}_m \mathrm{tr}\left(\bar{\boldsymbol{\Phi}}_{m,m} \boldsymbol{T}'_m \right)}{(1/\bar{I}) \left(\mathrm{tr}\left(\bar{\boldsymbol{\Phi}}_{m,m} \boldsymbol{T}_m \right) \right)^2}, & m = n, \\ 0, & m \neq n, \end{cases} \tag{21}$$

where

$$\begin{aligned}
\boldsymbol{T}'_m &= \boldsymbol{T}_m \left(\frac{1}{\bar{I}} \sum_{n=1, n \neq m}^{\bar{I}} \lambda_n \bar{\boldsymbol{\Phi}}_{m,n} \frac{\delta'_n}{(1 + \delta_n)^2} + \boldsymbol{I}_{M_{\lceil m/I \rceil}} \right) \boldsymbol{T}_m, \\
\delta'_n &= \frac{1}{\bar{I}} \mathrm{tr}\left(\lambda_n \bar{\boldsymbol{\Phi}}_{m,n} \boldsymbol{T}'_m \right).
\end{aligned}$$

Proof: The proof is given in Section 8.2 of the Appendix. □

To compute the downlink transmit power, the extended coupling matrix $\boldsymbol{Q}$ is approximated as

$$\tilde{\boldsymbol{Q}} = \begin{bmatrix} \tilde{\boldsymbol{D}} \tilde{\boldsymbol{G}} & \tilde{\boldsymbol{D}} \boldsymbol{1}_{\bar{I}} \\ \dfrac{1}{\sum_{m=1}^{\bar{I}} \lambda_m} \tilde{\boldsymbol{v}}^{\mathrm{T}} \tilde{\boldsymbol{D}} \tilde{\boldsymbol{G}} & \dfrac{1}{\sum_{m=1}^{\bar{I}} \lambda_m} \tilde{\boldsymbol{v}}^{\mathrm{T}} \tilde{\boldsymbol{D}} \boldsymbol{1}_{\bar{I}}. \end{bmatrix} \tag{22}$$

Thus, the algorithm to compute the optimal downlink transmit power $\boldsymbol{p}$ is given in Algorithm 2 (Fig. 2), where $\boldsymbol{f}_{\max}$ is the maximum eigenvector of the extended coupling matrix of $\tilde{\boldsymbol{Q}}$, ς is the update step, $\boldsymbol{g}$ is the subgradient of the virtual noise vector $\boldsymbol{v}$, ε denotes the threshold of inner iteration loop, and δ denotes the threshold of outer iteration loop.

The convexity of problem (8) ensures the convergence of updating $\boldsymbol{v}[l+1]$ by the subgradient method, i.e. the outer iteration loop is guaranteed to converge. According to the results on deterministic equivalents [12], the virtual uplink transmit power λ and the transmit power $\boldsymbol{p}$ converge to deterministic point in a massive MIMO system, i.e. the inner iteration loop is guaranteed to converge too.

In Algorithm 2 (Fig. 2), each BS updates the virtual uplink user power only using statistical CSI in step 3 and then updates correspondingly the downlink user power via the extended coupling matrix which only requires statistical CSI in step 7. In other words, $\boldsymbol{\lambda}$ and $\boldsymbol{p}$ can be updated at a long-term timescale. Therefore, Algorithm 2 (Fig. 2) operates on the order of tens of seconds or more (at the same timescale as the variation of the long-term channel statistics) and thus the implementation complexity is greatly reduced. The specific cooperation overhead

Algorithm 2

1: Initialise $\mathbf{v}[0] \in R_{+}^{\bar{I}}$, $i = 0$;

2: Initialise $\boldsymbol{\lambda}[0] \in R_{+}^{\bar{I}}$ such that $\sum_{m=1}^{\bar{I}} \lambda_m[0] \le \sum_{j=1}^{K} v_j[i]P_j$, $l = 0$;

3: Let $l = l + 1$, compute $\boldsymbol{\Upsilon}_m$ with $\mathbf{v}[i], \boldsymbol{\lambda}[l-1]$, then uplink power $\boldsymbol{\lambda}[l]$ with $\lambda_m[l] = \frac{1}{\boldsymbol{\Upsilon}_m}\lambda_m[l-1]$, then normalise $\boldsymbol{\lambda}[l]$ as $\boldsymbol{\lambda}[l] \leftarrow \frac{\sum_{j=1}^{K} v_j[i]P_j}{\sum_{m=1}^{\bar{I}} \lambda_m[l]}\boldsymbol{\lambda}[l]$, and repeat this step until convergence;

4: According to (20), (21), (22), compute $\tilde{\mathbf{G}}_{m,n}$, $\tilde{\mathbf{D}}_{m,n}$ and $\tilde{\mathbf{Q}}$, and update downlink power $\mathbf{p}$:

5: Let $i = i + 1$, optimise $\mathbf{v}[i]$: $\mathbf{v}[i] = \mathbf{v}[i-1] - \varsigma\mathbf{g}$ with subgradient method, if $\|\mathbf{v}[i] - \mathbf{v}[i-1]\| > \delta$, return to step 2; otherwise, the iteration stops.

Fig. 2 *Multicell MU-MISO power allocation optimisation*

Table 1 Overhead of cooperation

Step	Exchange of inter-BS
3	$\lambda_m d_{m,m} R_{m,m}$, $\lambda_n d_{m,n} \boldsymbol{R}_{m,n}$
7	$\boldsymbol{\lambda}$, $d_{m,m}\boldsymbol{R}_{m,m}$, $d_{n,m}\boldsymbol{R}_{n,m}$
$\boldsymbol{w}_m^{\text{opt}}$	$\boldsymbol{\lambda}$, local CSI

of Algorithm 2 (Fig. 2) is summarised in Table 1. In contrast, the power update in Algorithm 1 (Fig. 1) is on the order of milliseconds to track the instantaneous channel effect. Thus, Algorithm 1 (Fig. 1) requires a large amount of instantaneous power update to compute the optimal solution [12].

5 Low-complexity beamforming

In the massive MIMO system, the computation of matrix inversion in the MMSE beamformer will grow with the system dimension, which has become a major hurdle in implementation of the proposed algorithm. To solve it, we provide a low-complexity calculator of the beamforming vectors based on TPE approach. In order to guarantee the performance of such a low-complexity solution, we derive the equivalent form of the uplink SINR achieved by the TPE beamforming. Then, a new optimisation problem is formulated to optimise the polynomial coefficients of TPE beamforming, which only requires the statistical CSI. For notation convenience, here we define some new symbols as follows

$$\boldsymbol{H} = \left(\sqrt{\lambda_1}\bar{\boldsymbol{h}}_{m,1},\ \ldots,\ \sqrt{\lambda_m}\bar{\boldsymbol{h}}_{m,m},\ \ldots,\ \sqrt{\lambda_{\bar{I}}}\bar{\boldsymbol{h}}_{m,\bar{I}}\right). \tag{23}$$

The MMSE beamformer in (10) is approximated by the truncated polynomial expansion [23, 24]

$$\boldsymbol{w}_m^{\text{TPE}} = \sum_{l=0}^{N-1} u_l \left(\frac{1}{\bar{I}}\boldsymbol{H}_m\boldsymbol{H}_m^{\text{H}}\right)^l \bar{\boldsymbol{h}}_{m,m}. \tag{24}$$

where $\boldsymbol{H}_m$ denotes the matrix that is obtained by removing $\sqrt{\lambda_m}\bar{\boldsymbol{h}}_{m,m}$ from $\boldsymbol{H}$, $u_0, \ldots, u_{N-1}$ is a sequence of real design parameters and N is the TPE order. Plugging (24) in the expression of the virtual uplink SINR (9) of user-$(\lceil m/I \rceil, m - I\lfloor m/I \rfloor)$, we have

$$\gamma_m = \frac{\boldsymbol{u}^{\text{H}}\lambda_m\boldsymbol{A}_m\boldsymbol{u}}{\boldsymbol{u}^{\text{H}}\left(\sum_{n=1,n\ne m}^{\bar{I}}\lambda_n\boldsymbol{B}_{m,n} + v_{\lceil m/I \rceil}\boldsymbol{C}_m\right)\boldsymbol{u}}, \tag{25}$$

Algorithm 3

Initialise

$$Z_{m,n}^{(0,0)} \leftarrow \frac{1}{\bar{I}} tr\left(\bar{\boldsymbol{\Phi}}_{m,n}\mathbf{I}_{M_{\lceil \frac{m}{I} \rceil}}\bar{\boldsymbol{\Phi}}_{m,m}\right)$$

for $l = 1 \to p$

$$Z_{m,n}^{(l,0)} \leftarrow \frac{1}{\bar{I}} tr\left(\bar{\boldsymbol{\Phi}}_{m,n}\boldsymbol{\Delta}_l\bar{\boldsymbol{\Phi}}_{m,m}\right) - \sum_{i=1}^{l}\binom{l}{i} i\beta_{n,i-1}Z_{m,n}^{(l-i,0)}$$

$$Z_{m,n}^{(0,l)} \leftarrow \frac{1}{\bar{I}} tr\left(\bar{\boldsymbol{\Phi}}_{m,n}\boldsymbol{\Delta}_l\bar{\boldsymbol{\Phi}}_{m,m}\right) - \sum_{i=1}^{l}\binom{l}{i} i\beta_{n,i-1}Z_{m,n}^{(0,l-i)}$$

end

for $l = 1 \to p$

  for $k = 1 \to p$

$$\begin{aligned} Z_{m,n}^{(l,k)} \leftarrow & \frac{1}{\bar{I}} tr\left(\bar{\boldsymbol{\Phi}}_{m,n}\boldsymbol{\Delta}_l\bar{\boldsymbol{\Phi}}_{m,m}\boldsymbol{\Delta}_k\right) \\ & - \sum_{i=1}^{l}\binom{l}{i} i\beta_{n,i-1}Z_{m,n}^{(l-i,k)} \\ & - \sum_{j=1}^{k}\binom{k}{j} j\beta_{n,j-1}Z_{m,n}^{(l,k-j)} \\ & - \sum_{i=1}^{l}\sum_{j=1}^{k}\binom{l}{i}\binom{k}{j} ij\beta_{n,i-1}\beta_{n,j-1}Z_{m,n}^{(l-i,k-j)} \end{aligned}$$

  end

end

Fig. 3 *Iterative algorithm for computing $Z_{m,n}^{(l,k)}$ $(l = 1, \ldots, p,\ k = 1, \ldots, p)$*

where $\boldsymbol{u} = (u_0, \ldots, u_{N-1})^{\mathrm{T}}$, $\boldsymbol{A}_m \in \mathbb{C}^{N\times N}$, $\boldsymbol{B}_{m,n} \in \mathbb{C}^{N\times N}$, $\boldsymbol{C}_m \in \mathbb{C}^{N\times N}$, $l = 0, \ldots, N-1$, $k = 0, \ldots, N-1$ and the TPE matrices $\boldsymbol{A}_m$, $\boldsymbol{B}_{m,n}$, $\boldsymbol{C}_m$ are described as follows

$$[\boldsymbol{A}_m]_{l,k} = \bar{\boldsymbol{h}}_{m,m}^{\mathrm{H}}\left(\frac{1}{\bar{I}}\boldsymbol{H}_m\boldsymbol{H}_m^{\mathrm{H}}\right)^l \bar{\boldsymbol{h}}_{m,m}\bar{\boldsymbol{h}}_{m,m}^{\mathrm{H}}\left(\frac{1}{\bar{I}}\boldsymbol{H}_m\boldsymbol{H}_m^{\mathrm{H}}\right)^k \bar{\boldsymbol{h}}_{m,m}, \tag{26}$$

$$[\boldsymbol{B}_{m,n}]_{l,k} = \bar{\boldsymbol{h}}_{m,m}^{\mathrm{H}}\left(\frac{1}{\bar{I}}\boldsymbol{H}_m\boldsymbol{H}_m^{\mathrm{H}}\right)^l \bar{\boldsymbol{h}}_{m,n}\bar{\boldsymbol{h}}_{m,n}^{\mathrm{H}}\left(\frac{1}{\bar{I}}\boldsymbol{H}_m\boldsymbol{H}_m^{\mathrm{H}}\right)^k \bar{\boldsymbol{h}}_{m,m}, \tag{27}$$

$$[\boldsymbol{C}_m]_{l,k} = \bar{\boldsymbol{h}}_{m,m}^{\mathrm{H}}\left(\frac{1}{\bar{I}}\boldsymbol{H}_m\boldsymbol{H}_m^{\mathrm{H}}\right)^{l+k} \bar{\boldsymbol{h}}_{m,m}. \tag{28}$$

Thus, we can optimise the asymptotic uplink SINR with respect to the polynomial coefficients $\boldsymbol{u} = (u_0, \ldots, u_{N-1})^{\mathrm{T}}$ by formulating an optimisation problem expressed as follows

$$\begin{cases} \underset{\boldsymbol{u}}{\text{maximise}} & \gamma_m = \dfrac{\boldsymbol{u}^{\mathrm{H}}\lambda_m\boldsymbol{A}_m\boldsymbol{u}}{\boldsymbol{u}^{\mathrm{H}}\left(\sum_{n=1,n\neq m}^{\bar{I}}\lambda_n\boldsymbol{B}_{m,n} + \nu_{\lceil m/I\rceil}\boldsymbol{C}_m\right)\boldsymbol{u}}, \\ \text{s.t.} & \boldsymbol{u}^{\mathrm{H}}\boldsymbol{C}_m\boldsymbol{u} = 1. \end{cases} \tag{29}$$

The following Lemma 2 discloses that the optimal solution $\boldsymbol{u}_{\mathrm{opt}}$ of the above problem.

Lemma 2: Let $\boldsymbol{a}$ be an eigenvector corresponding to the maximum eigenvalue of $\boldsymbol{\Gamma}\lambda_m\boldsymbol{A}_m\boldsymbol{\Gamma}$ and

$$\boldsymbol{u}^{\mathrm{opt}} = \left(\sum_{n=1,n\neq m}^{\bar{I}}\lambda_n\boldsymbol{B}_{m,n} + \nu_{\lceil m/I\rceil}\boldsymbol{C}_m\right)^{-(1/2)}\boldsymbol{a}/\alpha,$$

where $\Gamma = \left(\sum_{n=1,n\neq m}^{\bar{I}}\lambda_n\boldsymbol{B}_{m,n} + \nu_{\lceil m/I\rceil}\boldsymbol{C}_m\right)^{-(1/2)}$ and the scaling factor α is given by

$$\alpha = \left\|\boldsymbol{C}_m^{1/2}\left(\sum_{n=1,n\neq m}^{\bar{I}}\lambda_n\boldsymbol{B}_{m,n} + \nu_{\lceil m/I\rceil}\boldsymbol{C}_m\right)^{-(1/2)}\boldsymbol{a}\right\|.$$

Proof: The result follows trivially by Boyd and Vandenberghe [25], so the proof is omitted here. □

Since $\boldsymbol{A}_m \in \mathbb{C}^{N\times N}$, $\boldsymbol{B}_{m,n} \in \mathbb{C}^{N\times N}$, $\boldsymbol{C}_m \in \mathbb{C}^{N\times N}$ are of finite dimensions, we derive deterministic equivalentence for each of their elements using the resolvent matrix. By introducing the following random functions in t, we have

$$X_m(t) = \frac{1}{\bar{I}}\bar{\boldsymbol{h}}_{m,m}^{\mathrm{H}}\left(\frac{t}{\bar{I}}\boldsymbol{H}_m\boldsymbol{H}_m^{\mathrm{H}} + \boldsymbol{I}_{M_{\lceil m/I\rceil}}\right)^{-1}\bar{\boldsymbol{h}}_{m,m}, \tag{30}$$

$$Z_{m,n}(t_1, t_2) = \frac{1}{\bar{I}}\bar{\boldsymbol{h}}_{m,m}^{\mathrm{H}}\boldsymbol{\Sigma}(t_1)\bar{\boldsymbol{h}}_{m,n}\bar{\boldsymbol{h}}_{m,n}^{\mathrm{H}}\boldsymbol{\Sigma}(t_2)\bar{\boldsymbol{h}}_{m,m}, \tag{31}$$

Table 2 Simulation parameters

Parameters	Values
distance of inter-BS	1 km
bandwidth of channel	10 MHz
path loss (in dB) model	$15.3 + 37.6\log_{10} d$(d: metre)
antenna gain	15 dBi
log-normal shadowing	8 dB
noise power spectral density	−162 dBm/Hz
noise figure	9 dB

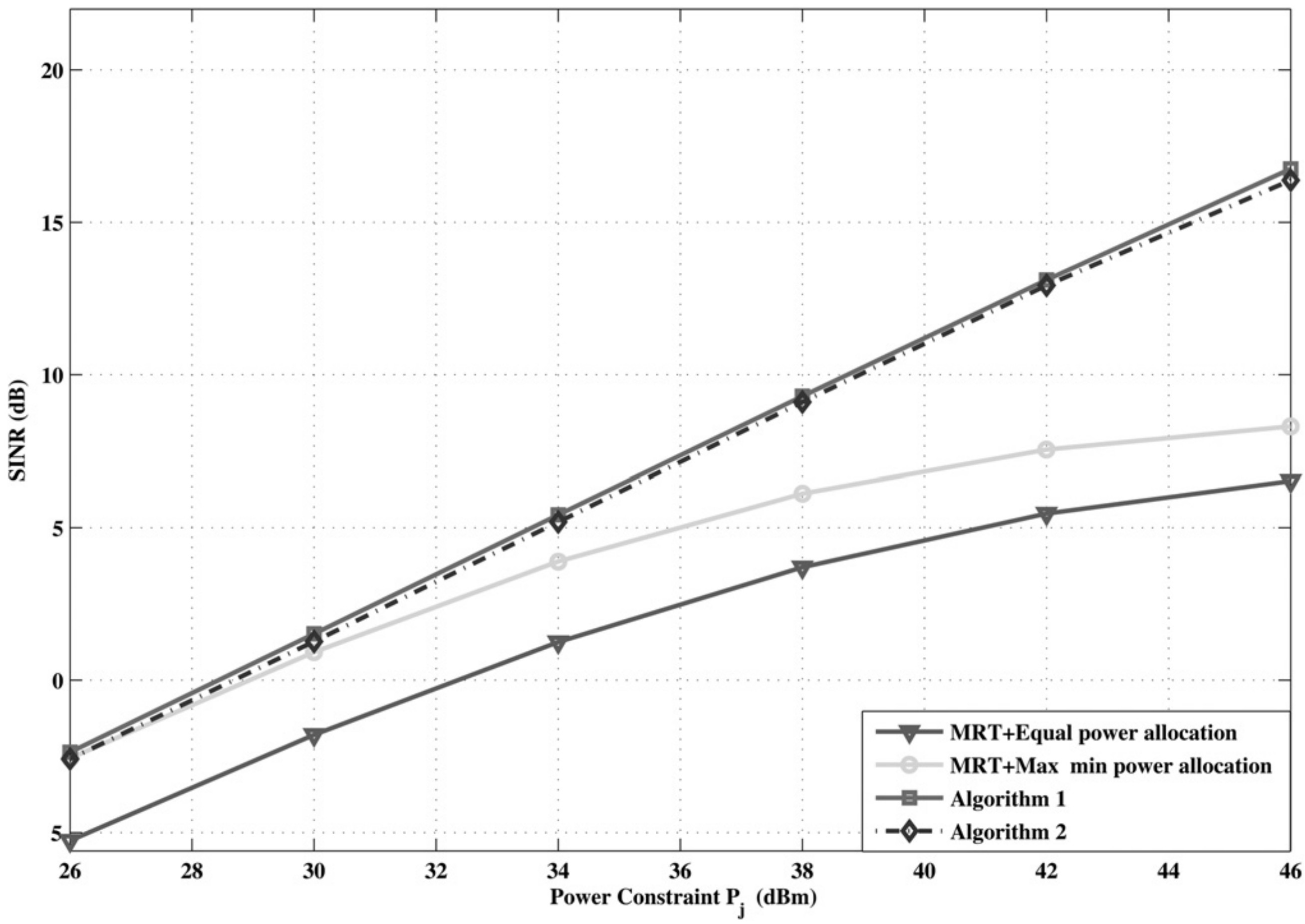

Fig. 4 *SINR performance achieved by Algorithms 1 and 2 (Figs. 1 and 2), and the MRT against per BS power constraint P (M = 64, I = 4, K = 3)*

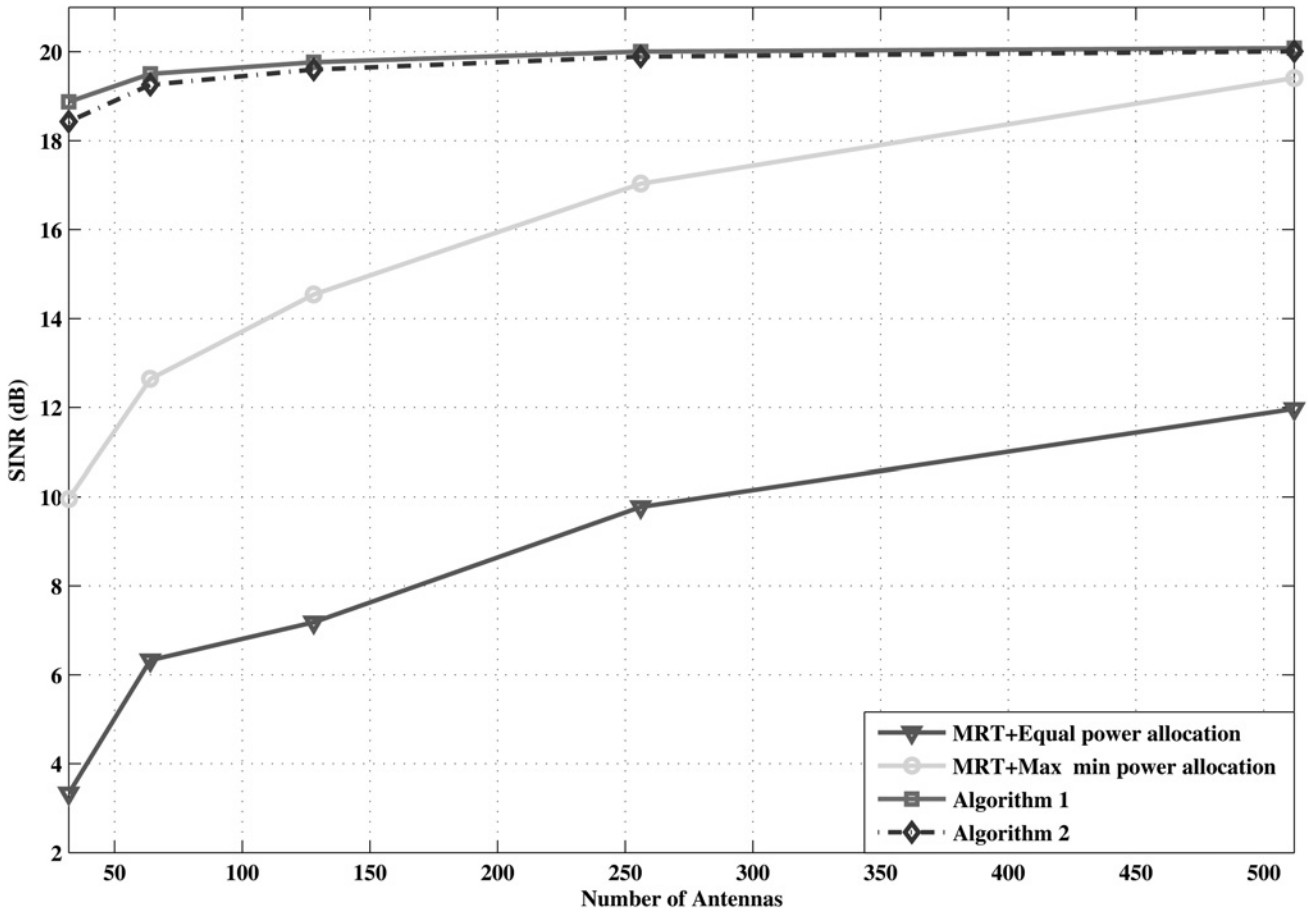

Fig. 5 *SINR performance achieved by Algorithms 1 and 2 (Figs. 1 and 2), and the MRT against the number of transmit antennas M (I = 4, K = 3, P = 46 dBm)*

where $\boldsymbol{\Sigma}(t) = \left((t/\bar{I})\boldsymbol{H}_m\boldsymbol{H}_m^{\mathrm{H}} + \boldsymbol{I}_{M_{\lceil m/I \rceil}}\right)^{-1}$. By taking derivations of (30) and (31), we obtain

$$\left.\frac{\mathrm{d}^l X_m(t)}{\mathrm{d}t^l}\right|_{t=0} = (-1)^l l!\frac{1}{\bar{I}}\bar{\boldsymbol{h}}_{m,m}^{\mathrm{H}}\left(\frac{1}{\bar{I}}\boldsymbol{H}_m\boldsymbol{H}_m^{\mathrm{H}}\right)^l \bar{\boldsymbol{h}}_{m,m}, \tag{32}$$

$$\begin{aligned}\left.\frac{\partial^l\partial^k Z_{m,n}(t_1, t_2)}{\partial t_1^l \partial t_2^k}\right|_{t_1=0,t_2=0} \\ = (-1)^{l+k} l!k!\frac{1}{\bar{I}}\bar{\boldsymbol{h}}_{m,m}^{\mathrm{H}}\left(\frac{1}{\bar{I}}\boldsymbol{H}_m\boldsymbol{H}_m^{\mathrm{H}}\right)^l \bar{\boldsymbol{h}}_{m,n}\bar{\boldsymbol{h}}_{m,n}^{\mathrm{H}}\left(\frac{1}{\bar{I}}\boldsymbol{H}_m\boldsymbol{H}_m^{\mathrm{H}}\right)^k \bar{\boldsymbol{h}}_{m,m}.\end{aligned} \tag{33}$$

Plugging (32) and (33) into (26)–(28), we have

$$[\boldsymbol{A}_m]_{l,k} = \frac{\bar{I}^2(-1)^{l+k}}{l!k!}\left.\frac{\mathrm{d}^l X_m(t)}{\mathrm{d}t^l}\right|_{t=0}\left.\frac{\mathrm{d}^k X_m(t)}{\mathrm{d}t^k}\right|_{t=0}, \tag{34}$$

$$[\boldsymbol{B}_{m,n}]_{l,k} = \frac{\bar{I}(-1)^{l+k}}{l!k!}\left.\frac{\partial^l\partial^k Z_{m,n}(t_1, t_2)}{\partial t_1^l\partial t_2^k}\right|_{t_1=0,t_2=0}, \tag{35}$$

$$[\boldsymbol{C}_m]_{l,k} = \frac{\bar{I}(-1)^{l+k}}{(l+k)!}\left.\frac{\mathrm{d}^{l+k}X_m(t)}{\mathrm{d}t^{l+k}}\right|_{t=0}. \tag{36}$$

According to Lemmas 3 and 4 in the Appendix and the Rank-1 perturbation lemma in [26], (30) can be transformed into the following form

$$X_m(t) \to \frac{1}{\bar{I}}\mathrm{tr}\left(\bar{\boldsymbol{\Phi}}_{m,m}\left(\frac{t}{\bar{I}}\boldsymbol{H}\boldsymbol{H}^{\mathrm{H}} + \boldsymbol{I}_{M_{\lceil m/I \rceil}}\right)^{-1}\right) \to \frac{1}{\bar{I}}\mathrm{tr}\left(\bar{\boldsymbol{\Phi}}_{m,m}\boldsymbol{\Delta}(t)\right), \tag{37}$$

where

$$\boldsymbol{\Delta}(t) = \left(\boldsymbol{I}_{M_{\lceil m/I \rceil}} + \frac{1}{\bar{I}}\sum_{n=1}^{\bar{I}}\lambda_n\bar{\boldsymbol{\Phi}}_{m,n}\frac{t\boldsymbol{I}_{M_{\lceil m/I \rceil}}}{1 + t\beta_n(t)}\right)^{-1}.$$

$$\beta_n(t) = \frac{1}{\bar{I}}\mathrm{tr}\left(\lambda_n\boldsymbol{\Phi}_{m,n}\boldsymbol{\Delta}(t)\right).$$

Thus the derivatives of $X_m(t)$ can be calculated as follows

$$\frac{\mathrm{d}^l X_m(t)}{\mathrm{d}t^l} \to \frac{1}{\bar{I}}\mathrm{tr}\left(\bar{\boldsymbol{\Phi}}_{m,m}\boldsymbol{\Delta}_l(t)\right),$$

where $\boldsymbol{\Delta}_l(t)$ is the derivatives of $\boldsymbol{\Delta}(t)$ and the corresponding derivatives of $\boldsymbol{\Delta}$ can be computed using the iterative algorithm in [27]. By substituting the derivatives of $X_m(t)$ into (34) and (36), we can obtain the elements $[\boldsymbol{A}_m]_{l,k}$ and $[\boldsymbol{C}_m]_{l,k}$ of the TPE matrices $\boldsymbol{A}_m$ and $\boldsymbol{C}_m$ with (34) and (36), respectively. In what follows we study the derivatives of $Z_{m,n}(t_1, t_2)$ to obtain the TPE matrix $\boldsymbol{B}_{m,n}$.

Theorem 2: In the large-scale system, assuming that M and I tend to infinity and

$$0 < \liminf\frac{I}{M} \le \limsup\frac{I}{M} < +\infty,$$

IET Commun., 2016, Vol. 10, Iss. 17, pp. 2380–2390

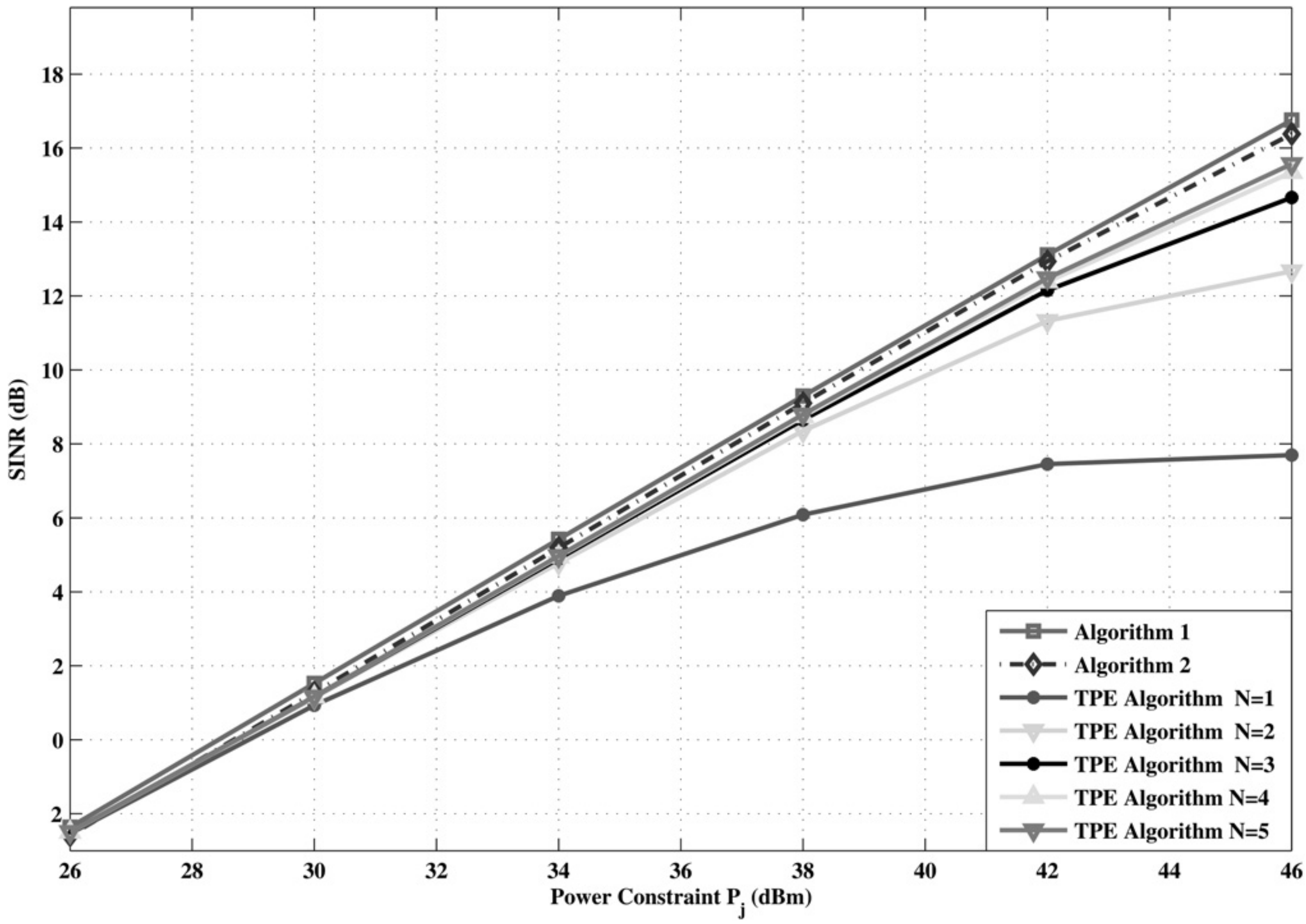

Fig. 6 *SINR performance achieved by the TPE beamformer, Algorithms 1 and 2 (Figs. 1 and 2) against per BS power constraints P_j ($M = 64$, $I = 4$, $K = 3$)*

then it holds that

$$Z_{m,n}(t_1, t_2) - \frac{1}{I}\frac{\bar{\boldsymbol{h}}_{m,n}^{\mathrm{H}}\boldsymbol{Q}_n(t_2)}{1 + t_2\beta_n(t_2)}\bar{\Phi}_{m,m}\frac{\boldsymbol{Q}_n(t_1)\bar{\boldsymbol{h}}_{m,n}}{1 + t_1\beta_n(t_1)} \xrightarrow[M\to\infty]{\text{a.s.}} 0, \tag{38}$$

where

$$\boldsymbol{Q}_n(t) = \left(\frac{t}{I}\boldsymbol{H}_{mn}\boldsymbol{H}_{mn}^{\mathrm{H}} + \boldsymbol{I}_M\right)^{-1}.$$

Proof: The proof is given in Section 8.3 of the Appendix. □

After some basic mathematical operations of (38) and using Lemma 3, we have

$$\begin{aligned} &Z_{m,n}(t_1, t_2) + Z_{m,n}(t_1, t_2)t_1\beta_n(t_1) + Z_{m,n}(t_1, t_2)t_2\beta_n(t_2) \\ &\quad + Z_{m,n}(t_1, t_2)t_1\beta_n(t_1)t_2\beta_n(t_2) \xrightarrow[M_{\lceil m/I\rceil}\to\infty]{\text{a.s.}} \frac{1}{I}\mathrm{tr}\left(\bar{\boldsymbol{\Phi}}_{m,n}\boldsymbol{\Delta}(t_2)\bar{\boldsymbol{\Phi}}_{m,m}\boldsymbol{\Delta}(t_1)\right). \end{aligned} \tag{39}$$

Computing the lth derivatives for t_1 and the kth derivatives for t_2 of (39), we have

$$\begin{aligned} Z_{m,n}^{(l,k)} &\to \frac{1}{I}\mathrm{tr}\left(\bar{\boldsymbol{\Phi}}_{m,n}\boldsymbol{\Delta}_l\bar{\boldsymbol{\Phi}}_{m,m}\boldsymbol{\Delta}_k\right). \\ &- \sum_{i=1}^{l}\binom{l}{i}i\beta_{n,i-1}Z_{m,n}^{(l-i,k)} - \sum_{j=1}^{k}\binom{k}{j}j\beta_{n,j-1}Z_{m,n}^{(l,k-j)} \\ &- \sum_{i=1}^{l}\sum_{j=1}^{k}\binom{l}{i}\binom{k}{j}ij\beta_{n,i-1}\beta_{n,j-1}Z_{m,n}^{(l-i,k-j)} \end{aligned} \tag{40}$$

where $Z_{m,n}^{(l,k)}$ represents the lth derivatives for t_1 and the kth derivatives for t_2 of $Z_{m,n}(t_1, t_2)$, $\boldsymbol{\Delta}_l$ and $\boldsymbol{\Delta}_k$ are the derivatives of $\boldsymbol{\Delta}$, $\beta_{n,i-1}$ and $\beta_{n,j-1}$ are the derivatives of β_n. The iterative algorithm of computing $Z_{m,n}(t_1, t_2)$ is summarised in Algorithm 3 (Fig. 3), then the element $[B_{m,n}]_{l,k}$ of the TPE matrix $B_{m,n}$ can be obtained by (35).

Remark 1: In the proposed TPE beamforming scheme, the large-dimension matrix inversion is approximated by truncated polynomial expansion. Thus its complexity of the large matrix inversion can be reduced from $\mathcal{O}\left(M_j^{2.736}\right)$ to $\mathcal{O}\left(N^{2.736}\right)$, where N is the order of the truncated polynomial expansions. Note that N increases with the quality of requirements for QoS and usually does not need to scale with the system dimension. For instance, our numerical results in Section 6 show that $N = 5$ is sufficient to achieve a near optimal performance for the case $M_j = 64$. Although the polynomial coefficients in (26)–(28) depend on the instantaneous CSI, we apply the random function to compute the asymptotic coefficients which only requires the statistical CSI and has ignorable performance loss especially when the number of antennas tends to infinity, meanwhile it also reduces the backhaul overhead of CSI collection.

6 Simulation results

In this section, the performance of the proposed algorithms is investigated via numerical examples. We consider a cluster of three cells with inter-BS distance of 1 km. Each cell consists one multiple-antenna BS and a plurality of single-antenna users. All users randomly locate in the cell edge and its distance away from the BS is no less than 400 m. The path loss (in dB) model is assumed with $15.3 + 37.6\log_{10} d$ for distance d in metres and the shadow fading follows the distribution $\mathcal{N}(0,\ 8\,\text{dB})$. For simulation convenience, each BS has the same number of transmit antenna M

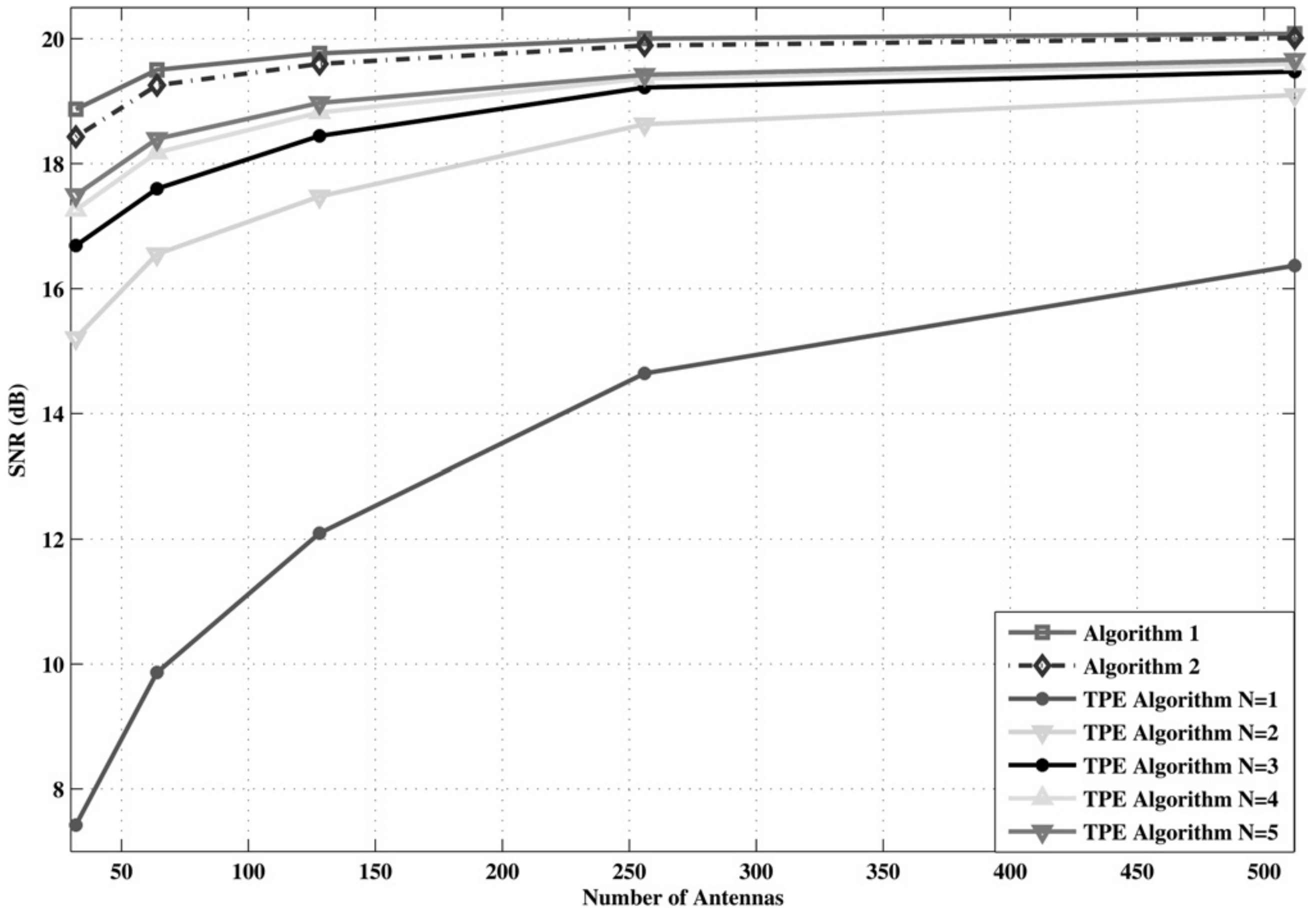

Fig. 7 *SINR performance achieved by the TPE beamformer, Algorithms 1 and 2 (Figs. 1 and 2) against the number of transmit antennas M (I = 4, K = 3, P = 46 dBm)*

and the covariance matrix is given as follows

$$[\boldsymbol{R}_{m,l,k}]_{i,j} = \begin{cases} r^{j-i}, & i < j, \\ (r^{i-j})^*, & i \geq j, \end{cases} \tag{41}$$

where $i = 1, 2, \ldots, M$, $j = 1, 2, \ldots, M$, $r = 0.6$. The simulation parameters are summarised in Table 2. For comparison, the conventional maximum ratio transmission (MRT) scheme is also simulated, where both equal power allocations among the beamforming vectors and max–min SINR optimised power allocation among the beamforming vectors are considered.

Fig. 4 illustrates the SINR performance achieved by several multicell beamforming algorithms including the proposed algorithms and the conventional MRT scheme, for the configuration $M = 64$ and $I = 4$. The results show that the proposed Algorithms 1 (Fig. 1) and 2 (Fig. 2) both significantly outperform the MRT algorithm employing equal power allocation or max–min power allocation, in terms of the average SINR, especially at the high transmit power regime. It is also seen that the performance of the proposed Algorithm 2 (Fig. 2) is very close to that of the proposed Algorithm 1 (Fig. 1) in a wide range of transmit power, verifying the effectiveness of the proposed Algorithm 2 (Fig. 2) which has much lower complexity and backhaul overhead.

Fig. 5 shows the SINR performance of the above algorithms with the varying number of antennas M at the BS, for the configuration $P = 46$ dBm and $I = 4$. The results reveal that the proposed Algorithm 2 (Fig. 2) is achieving more close SINR performance to the proposed Algorithm 1 (Fig. 1) as the number of transmit antennas increases. This confirms that our proposed Algorithm 2 (Fig. 2) is asymptotically optimal in the massive MIMO system. At the same time, one can see that our proposed algorithms have a large gain over the MRT algorithm when the number of transmit antennas is not large enough. One also notes that the performance improvement becomes smaller and smaller as the number of antennas increases in large-scale MIMO wireless communication system [3] [We would like to explore in detail the tradeoff between performance and hardware cost. Nonetheless, it falls out of the scope of current work.].

Fig. 6 illustrates the impact of employing TPE beamforming of different order N on the performance of the proposed algorithms, for the configuration $M = 64$ and $I = 4$. It is shown that the performance of TPE beamforming algorithm is getting closer to that of the proposed Algorithm 2 (Fig. 2) as the TPE order N increasing. In particular, at the low transmit power regime, a small value of N such as $N = 5$ suffers very marginal performance loss. The results show that the performance loss caused by TPE increases with the transmit power constraint, but even in the high transmit power regime, the TPE beamforming with $N = 5$ obtains a large portion of the optimal performance, while having much reduced computational complexity compared with Algorithm 2 (Fig. 2).

Fig. 7 further shows the SINR performance achieved by the low-complexity TPE beamforming algorithm with the varying number of transmit antennas M under configuration $P = 46$ dBm. Similar to the results shown in Fig. 6, one can see that the performance of TPE beamforming algorithm is getting closer to the optimal one with the increasing order N. In particular, when the number of transmit antennas M is becoming larger, the results show that a smaller value of N is needed to get the same portion of the optimal performance. This implies that our TPE beamforming design is effective in a massive MIMO system.

7 Conclusions

In this paper, we have studied joint beamforming and power allocation for a multicell massive MIMO system with the objective of maximising the minimum SINR. By introducing some auxiliary variables, we first transformed the original downlink optimisation problem into an equivalent dual uplink optimisation problem where the optimal beamformers have analytic structure. An iterative algorithm was then developed to achieve its solution, but it depends on the instantaneous CSI. To address this issue, the random matrix theory was applied to generalise the uplink–downlink duality to an asymptotical form in which the solution conversion from the uplink to the downlink is only based on statistical CSI. Based on that, an efficient multicell beamforming solution was proposed to asymptotically achieve the max–min SINR solution, in which the power allocation is calculated on a long-term basis while the beamforming vector is obtained with a closed-form expression and on a short-term basis. Since the beamforming computation still involves a large matrix inversion and becomes computationally prohibitive as the number of antennas increase infinitely, we have further proposed a low-complexity TPE beamformer scheme in which the large matrix inversion is efficiently approximated by the truncated polynomial expansions. To determine the polynomial coefficients of the TPE beamformer efficiently, we first derived the equivalent form of the uplink SINR achieved by the TPE beamforming, based on which we then formulated an optimisation problem to calculate the polynomial coefficients based on statistical CSI. The effectiveness of the above proposals was validated via numerical results.

8 Acknowledgments

This work was supported by National Natural Science Foundation of China under Grants 61471120, 61422105, 61302097, and 61372101, the Fundamental Research Funds for the Central Universities under Grant 2242016K40099, and the Research Project of Jiangsu Province under Grants BK20130019, BE2015156 and BK20161428.

9 References

1 Marzetta, T.L.: 'Noncooperative cellular wireless with unlimited numbers of base station antennas', *IEEE Trans. Wirel. Commun.*, 2010, **9**, (11), pp. 3590–3600
2 Rusek, F., Persson, D., Lau, B., *et al.*: 'Scaling up MIMO: opportunities and challenges with very large arrays', *IEEE Signal Process. Mag.*, 2013, **30**, (1), pp. 40–60
3 Hoydis, J., Brink, S., Debbah, M.: 'Massive MIMO in the UL/DL of cellular networks: How many antennas do we need?', *IEEE J. Sel. Areas Commun.*, 2013, **31**, (2), pp. 160–171
4 Wagner, S., Couillet, R., Debbah, M., *et al.*: 'Large system analysis of linear precoding in correlated MISO broadcast channels under limited feedback', *IEEE Trans. Inf. Theory*, 2012, **58**, (7), pp. 4509–4537
5 Dahrouj, H., Yu, W.: 'Coordinated beamforming for the multicell multi-antenna wireless system', *IEEE Trans. Wirel. Commun.*, 2010, **9**, (5), pp. 1748–1759
6 Hoydis, J., Brink, S., Debbah, M.: 'Comparison of linear precoding schemes for downlink massive MIMO'. Proc. IEEE Int. Conf. on Communications (ICC), 2012, pp. 2135–2139
7 Yu, W., Lan, T.: 'Transmitter optimization for the multiantenna downlink with per-antenna power constraints', *IEEE Trans. Signal Process.*, 2007, **55**, (6), pp. 2646–2260
8 Yang, W., Xu, G.: 'Optimal downlink power assignment for smart antenna systems'. IEEE Int. Conf. Acoustic, Speech and Signal Processing (ICASSP), May 1998, vol. 6, pp. 3337–3340
9 Schubert, M., Boche, H.: 'Solution of the multiuser downlink beamforming problem with individual SINR constraints', *IEEE Trans. Veh. Technol.*, 2004, **53**, (1), pp. 18–28
10 He, S., Huang, Y., Yang, L., *et al.*: 'A multi-cell beamforming design by uplink-downlink max-min SINR duality', *IEEE Trans. Wirel. Commun.*, 2012, **11**, (8), pp. 2858–2867
11 Zakhour, R., Hanly, S.: 'Base station cooperation on the downlink: Large system analysis', *IEEE Trans. Inf. Theory*, 2012, **58**, (4), pp. 2079–2106
12 Huang, Y., Tan, C., Rao, B.: 'Joint beamforming and power control in coordinated multicell: max-min duality, effective network and large system transition', *IEEE Trans. Wirel. Commun.*, 2013, **12**, (6), pp. 2730–2742
13 Hachem, W., Khorunzhy, O., Loubaton, P., *et al.*: 'A new approach for capacity analysis of large dimensional multi-antenna channels', *IEEE Trans. Inf. Theory*, 2008, **54**, (9), pp. 3987–4004
14 Nguyen, V., Evans, J.: 'Multiuser transmit beamforming via regularized channel inversion: a large system analysis'. Proc. IEEE Global Communication Conf. (GLOBECOM), 2008
15 Kammoun, A., Kharouf, M., Hachem, W., *et al.*: 'A central limit theorem for the SINR at the LMMSE estimator output for large dimensional signals', *IEEE Trans. Inf. Theory*, 2009, **55**, (11), pp. 5048–5063
16 Couillet, R., Debbah, M.: 'Random matrix methods for wireless communications' (Cambridge University Press, New York, NY, USA, 2011, 1st edn.)
17 Foschini, G., Miljanic, Z.: 'A simple distributed autonomous power control algorithm and its convergence', *IEEE Trans. Veh. Technol.*, 1993, **42**, (4), pp. 641–646
18 Yates, R.: 'A framework for uplink power control in cellular radio systems', *IEEE J. Sel. Areas Commun.*, 1995, **13**, (7), pp. 1341–1347
19 Bannour, A., Ammari, M., Sun, Y., *et al.*: 'Duality of transmit antennas and subcarriers in massive MIMO-OFDM downlink system', *IET Electron. Lett.*, 2015, **51**, (14), pp. 1115–1117
20 Ngo, H., Larsson, D., Marzetta, T.: 'Energy and spectral efficiency of very large multiuser MIMO systems', *IEEE Trans. on Commun.*, 2013, **61**, (4), pp. 1436–1449
21 Mohammed, S., Larsson, D.: 'Per-antenna constant envelope precoding for large multi-user MIMO systems', *IEEE Trans. Commun.*, 2013, **61**, (3), pp. 1509–1071
22 Zhang, X., Lee, J.: 'Low complexity MIMO scheduling with channel decomposition using capacity upperbound', *IEEE Trans. Commun.*, 2008, **56**, pp. 871–876
23 Zarei, S., Gerstacker, W., Muller, R., *et al.*: 'Low-complexity linear precoding for downlink large-scale MIMO systems'. Proc. IEEE Int. Symp. Personal, Indoor and Mobile Radio Communication (PIMRC), 2013
24 Muller, A., Kammoun, A., Bjornson, E., *et al.*: 'Linear precoding based on polynomial expansion: reducing complexity in massive MIMO', *EURASIP J. Wirel. Commun. Netw.*, 2016, **2016**, p. 63
25 Boyd, S., Vandenberghe, L.: 'Convex optimization' (Cambridge University Press, 2004)
26 Silver, J., Bai, Z.: 'On the empirical distribution of eigenvalues of a class of large dimensional random matrices', *J. Multivariate Anal.*, 1995, **54**, (2), pp. 175–192
27 Hoydis, J., Debbah, M., Kobayashi, M.: 'Asymptotic moments for interference mitigation in correlated fading channels'. Proc. Int. Symp. Information Theory (ISIT), 2011
28 Bai, Z., Silverstein, J.: 'No eigenvalue outside the support of the limiting spectral distribution of large dimensional sample covariance matrices', *Ann. Probab.*, 1998, **26**, (1), pp. 316–345
29 Kammoun, A., Muller, A., Bjornson, E., *et al.*: 'Linear precoding based on polynomial expansion: large-scale multi-cell MIMO systems', *IEEE J. Sel. Top. Signal Process.*, 2014, **8**, (5), pp. 316–345
30 Golub, G., Van Van Loan, C.: 'Matrix computations' (The Johns Hopkins University Press, 1996)

10 Appendices

10.1 Related lemmas

Lemma 3 [28]: Let $\boldsymbol{x} \sim \mathcal{CN}(0, \boldsymbol{I}_M)$ and $\boldsymbol{U} \in^{M\times M}$ Hermitian with bounded spectral norm whose elements are independent of $\boldsymbol{x}$, then $(1/M)\boldsymbol{x}^{\mathrm{H}}\boldsymbol{U}\boldsymbol{x} - (1/M)\mathrm{tr}\boldsymbol{U} \xrightarrow[M\lceil m/I \rceil \to \infty]{\text{a.s.}} 0$.

Lemma 4 [4]: Let $\boldsymbol{U} \in^{M\times M}$ Hermitian with bounded spectral norm, $\boldsymbol{H} \in^{M\times \bar{I}}$ be a random matrix with independent column vectors and the column of $\boldsymbol{H}$ satisfies $\boldsymbol{h}_n \sim \mathcal{CN}(0, \Phi_n)$. Then, for any $z > 0$ it holds that

$$\frac{1}{\bar{I}}\mathrm{tr}\big(\boldsymbol{U}\boldsymbol{\Sigma}(z)\big) - \frac{1}{\bar{I}}\mathrm{tr}(\boldsymbol{U}\boldsymbol{T}(z)) \xrightarrow[M\lceil m/I \rceil \to \infty]{\text{a.s.}} 0,$$

where

$$\boldsymbol{\Sigma}(z) = \big(\boldsymbol{H}\boldsymbol{H}^{\mathrm{H}} - z\boldsymbol{I}_M\big)^{-1},$$

$$\boldsymbol{T}(z) = \left(\frac{1}{\bar{I}}\sum_{n=1}^{\bar{I}}\frac{\boldsymbol{\Phi}_n}{1+\delta_n(z)} - z\boldsymbol{I}_M\right)^{-1},$$

$$\delta_n(z) = \frac{1}{\bar{I}}\mathrm{tr}\left(\boldsymbol{\Phi}_n\left(\frac{1}{\bar{I}}\sum_{k=1}^{\bar{I}}\frac{\boldsymbol{\Phi}_k}{1+\delta_k(z)} - z\boldsymbol{I}_M\right)^{-1}\right).$$

Lemma 5 [29]: Let $\boldsymbol{U} \in^{M\times M}$ Hermitian with bounded spectral norm, $\boldsymbol{H} \in^{M\times \bar{I}}$ be a random matrix with independent column vectors and the column of $\boldsymbol{H}$ satisfies $\boldsymbol{h}_n \sim \mathcal{CN}(0, \boldsymbol{\Phi}_n)$. Then, for any $t > 0$ it holds that

$$\frac{1}{\bar{I}}\mathrm{tr}\big(\boldsymbol{U}\boldsymbol{\Sigma}(t)\big) - \frac{1}{\bar{I}}\mathrm{tr}(\boldsymbol{U}\boldsymbol{\Delta}(t)) \xrightarrow[M\lceil m/I \rceil \to \infty]{\text{a.s.}} 0,$$

where

$$\boldsymbol{\Sigma}(t) = \left(\boldsymbol{I}_M + \frac{t\boldsymbol{H}\boldsymbol{H}^{\mathrm{H}}}{\bar{I}}\right)^{-1}.$$

$$\boldsymbol{\Delta}(t) = \left(\boldsymbol{I}_M + \frac{1}{\bar{I}}\sum_{n=1}^{\bar{I}} \lambda_n \boldsymbol{\Phi}_n \frac{t\boldsymbol{I}_M}{1+t\beta_n(t)}\right)^{-1}.$$

$$\beta_n(t) = \frac{1}{\bar{I}}\mathrm{tr}\left(\lambda_n \boldsymbol{\Phi}_n \boldsymbol{\Delta}(t)\right).$$

Lemma 6: The resolvent matrices of $\boldsymbol{H}_m$ and $\boldsymbol{H}_{mn}$ are denoted by $\boldsymbol{Q}(t) = \left((t/\bar{I})\boldsymbol{H}_m\boldsymbol{H}_m^{\mathrm{H}} + \boldsymbol{I}_M\right)^{-1}$ and $\boldsymbol{Q}_n(t) = \left((t/\bar{I})\boldsymbol{H}_{mn}\boldsymbol{H}_{mn}^{\mathrm{H}} + \boldsymbol{I}_M\right)^{-1}$, where $\boldsymbol{H}_m$ is obtained by removing the mth column $\boldsymbol{h}_m$ of $\boldsymbol{H}$ and $\boldsymbol{H}_{mn}$ does not include the mth column $\boldsymbol{h}_m$ and the nth column $\boldsymbol{h}_n$ of $\boldsymbol{H}$. Then it holds that

$$\boldsymbol{Q}(t) = \boldsymbol{Q}_n(t) - \frac{t}{\bar{I}}\frac{\lambda_n \boldsymbol{Q}_n(t)\boldsymbol{h}_n\boldsymbol{h}_n^{\mathrm{H}}\boldsymbol{Q}_n(t)}{1+(t/\bar{I})\lambda_n \boldsymbol{h}_n^{\mathrm{H}}\boldsymbol{Q}_n(t)\boldsymbol{h}_n},$$

and also

$$\boldsymbol{Q}(t)\boldsymbol{h}_n = \frac{\boldsymbol{Q}_n(t)\boldsymbol{h}_n}{1+(t/\bar{I})\lambda_n \boldsymbol{h}_n^{\mathrm{H}}\boldsymbol{Q}_n(t)\boldsymbol{h}_n}.$$

Proof: This follows from the Woodbury identity in [30]. □

10.2 Proof of Theorem 1

To mitigate the impact of the small-scale fading coefficients on the matrices $\boldsymbol{G}$ and $\boldsymbol{D}$, we firstly obtain the asymptotic determine expression of $\left\|\bar{\boldsymbol{h}}_{m,m}^{\mathrm{H}}\boldsymbol{w}_m\right\|^2$ and $\left\|\bar{\boldsymbol{h}}_{n,m}^{\mathrm{H}}\boldsymbol{w}_n\right\|^2$ based on the large dimension random theory. Then the asymptotic approximation of the extended coupling matrices $\boldsymbol{G}$ and $\boldsymbol{D}$ is obtained and is described as $\tilde{\boldsymbol{G}}$ and $\tilde{\boldsymbol{D}}$. Similar to the derivations of (18), we have the following two asymptotic deterministic expressions of $\left\|\bar{\boldsymbol{h}}_{m,m}^{H}\boldsymbol{w}_m\right\|^2$ and $\left\|\bar{\boldsymbol{h}}_{n,m}^{H}\boldsymbol{w}_n\right\|^2$. Employing Lemma 3 and the expression of beamformer in (10), we have

$$\left\|\bar{\boldsymbol{h}}_{m,m}^{H}\boldsymbol{w}_m\right\|^2 = \frac{\left(\bar{\boldsymbol{h}}_{m,m}^{\mathrm{H}}\left(\sum_{n\neq m}\lambda_n \bar{\boldsymbol{h}}_{m,n}\bar{\boldsymbol{h}}_{m,n}^{\mathrm{H}} + v_{\lceil m/I\rceil}\boldsymbol{I}_{M_{\lceil m/I\rceil}}\right)^{-1}\bar{\boldsymbol{h}}_{m,m}\right)^2}{\bar{\boldsymbol{h}}_{m,m}^{\mathrm{H}}\left(\sum_{n\neq m}\lambda_n \bar{\boldsymbol{h}}_{m,n}\bar{\boldsymbol{h}}_{m,n}^{\mathrm{H}} + v_{\lceil m/I\rceil}\boldsymbol{I}_{M_{\lceil m/I\rceil}}\right)^{-2}\bar{\boldsymbol{h}}_{m,m}}$$
$$\xrightarrow[M_{\lceil m/I\rceil}\to\infty]{\text{a.s.}} \frac{1}{\bar{I}}\frac{\left(\mathrm{tr}\left(\bar{\boldsymbol{\Phi}}_{m,m}\boldsymbol{T}_m\right)\right)^2}{\mathrm{tr}\left(\bar{\boldsymbol{\Phi}}_{m,m}\boldsymbol{T}'_m\right)}, \tag{42}$$

where

$$\bar{\boldsymbol{\Phi}}_{m,m} = \frac{\boldsymbol{\Phi}_{m,m}}{\sigma_m^2} = \frac{d_{m,m}}{\sigma_m^2 M_{\lceil m/I\rceil}}\boldsymbol{R}_{m,m}. \tag{43}$$

$$\boldsymbol{T}_m = \left(\frac{1}{\bar{I}}\sum_{n=1,n\neq m}^{\bar{I}}\lambda_n \bar{\boldsymbol{\Phi}}_{m,n}\frac{1}{1+\delta_n} + \frac{1}{\bar{I}}v_{\lceil m/I\rceil}\boldsymbol{I}_{M_{\lceil m/I\rceil}}\right)^{-1}.$$
$$\delta_n = \frac{1}{\bar{I}}\mathrm{tr}\left(\lambda_n \bar{\boldsymbol{\Phi}}_{m,n}\boldsymbol{T}_m\right), \tag{44}$$

$$\boldsymbol{T}'_m = \boldsymbol{T}_m\left(\frac{1}{\bar{I}}\sum_{n=1,n\neq m}^{\bar{I}}\lambda_n \bar{\boldsymbol{\Phi}}_{m,n}\frac{\delta'_n}{\left(1+\delta_n\right)^2} + \boldsymbol{I}_{M_{\lceil m/I\rceil}}\right)\boldsymbol{T}_m. \tag{45}$$

$$\delta'_n = \frac{1}{\bar{I}}\mathrm{tr}\left(\lambda_n \bar{\boldsymbol{\Phi}}_{m,n}\boldsymbol{T}'_m\right). \tag{46}$$

By using jointly the Rank-1 perturbation lemma [26] and Lemma 4, we have

$$\left\|\bar{\boldsymbol{h}}_{n,m}^{\mathrm{H}}\boldsymbol{w}_n\right\|^2 = \frac{\bar{\boldsymbol{h}}_{n,m}^{\mathrm{H}}\boldsymbol{\Xi}_n^{-1}\bar{\boldsymbol{h}}_{n,n}\bar{\boldsymbol{h}}_{n,n}^{\mathrm{H}}\boldsymbol{\Xi}_n^{-1}\bar{\boldsymbol{h}}_{n,m}}{\bar{\boldsymbol{h}}_{n,n}^{\mathrm{H}}\boldsymbol{\Xi}_n^{-2}\bar{\boldsymbol{h}}_{n,n}}$$
$$= \frac{\bar{\boldsymbol{h}}_{n,m}^{\mathrm{H}}\boldsymbol{\Theta}_n^{-1}\bar{\boldsymbol{h}}_{n,n}\bar{\boldsymbol{h}}_{n,n}^{\mathrm{H}}\boldsymbol{\Theta}_n^{-1}\bar{\boldsymbol{h}}_{n,m}}{\bar{\boldsymbol{h}}_{n,n}^{\mathrm{H}}\boldsymbol{\Xi}_n^{-2}\bar{\boldsymbol{h}}_{n,n}\left(1+\lambda_m \bar{\boldsymbol{h}}_{n,m}^{\mathrm{H}}\boldsymbol{\Theta}_n^{-1}\bar{\boldsymbol{h}}_{n,m}\right)^2}$$
$$\xrightarrow[M_{\lceil m/I\rceil}\to\infty]{\text{a.s.}} \frac{(1/\bar{I})\mathrm{tr}\left(\bar{\boldsymbol{\Phi}}_{n,n}\boldsymbol{T}_n\bar{\boldsymbol{\Phi}}_{n,m}\boldsymbol{T}_n\right)}{\mathrm{tr}\left(\bar{\boldsymbol{\Phi}}_{n,n}\boldsymbol{T}'_n\right)\left(1+\lambda_m(1/\bar{I})\mathrm{tr}\left(\bar{\boldsymbol{\Phi}}_{n,m}\boldsymbol{T}_n\right)\right)^2}, \tag{47}$$

where

$$\bar{\boldsymbol{\Phi}}_{n,n} = \frac{\boldsymbol{\Phi}_{n,n}}{\sigma_n^2} = \frac{d_{n,n}}{\sigma_n^2 M_{\lceil n/I\rceil}}\boldsymbol{R}_{n,n}, \tag{48}$$

$$\bar{\boldsymbol{\Phi}}_{n,m} = \frac{\boldsymbol{\Phi}_{n,m}}{\sigma_m^2} = \frac{d_{n,m}}{\sigma_m^2 M_{\lceil n/I\rceil}}\boldsymbol{R}_{n,m}, \tag{49}$$

$$\boldsymbol{\Xi}_n = \sum_{j\neq n}\lambda_j \bar{\boldsymbol{h}}_{n,j}\bar{\boldsymbol{h}}_{n,j}^{\mathrm{H}} + v_{\lceil n/I\rceil}\boldsymbol{I}_{M_{\lceil n/I\rceil}}, \tag{50}$$

$$\boldsymbol{\Theta}_n = \sum_{j\neq n,m}\lambda_j \bar{\boldsymbol{h}}_{n,j}\bar{\boldsymbol{h}}_{n,j}^{\mathrm{H}} + v_{\lceil n/I\rceil}\boldsymbol{I}_{M_{\lceil n/I\rceil}}. \tag{51}$$

Thus the elements of the matrices $\tilde{\boldsymbol{G}}$ and $\tilde{\boldsymbol{D}}$ can be calculated as follows

$$\tilde{\boldsymbol{G}}_{m,n} = \begin{cases} 0, & m=n, \\ \dfrac{(1/\bar{I})\mathrm{tr}\left(\bar{\boldsymbol{\Phi}}_{n,n}\boldsymbol{T}_n\bar{\boldsymbol{\Phi}}_{n,m}\boldsymbol{T}_n\right)}{\mathrm{tr}\left(\bar{\boldsymbol{\Phi}}_{n,n}\boldsymbol{T}'_n\right)\left(1+\lambda_m(1/\bar{I})\mathrm{tr}\left(\bar{\boldsymbol{\Phi}}_{n,m}\boldsymbol{T}_n\right)\right)^2}, & m\neq n, \end{cases} \tag{52}$$

$$\tilde{\boldsymbol{D}}_{m,n} = \begin{cases} \dfrac{\boldsymbol{Y}_m\ \mathrm{tr}\left(\bar{\boldsymbol{\Phi}}_{m,m}\boldsymbol{T}'_m\right)}{(1/\bar{I})\left(\mathrm{tr}\left(\bar{\boldsymbol{\Phi}}_{m,m}\boldsymbol{T}_m\right)\right)^2}, & m=n, \\ 0, & m\neq n, \end{cases} \tag{53}$$

10.3 Proof of Theorem 2

According to Lemmas 3, 5 and 6, (31) can be changed into

$$Z_{m,n}(t_1,t_2) = \frac{1}{\bar{I}}\bar{\boldsymbol{h}}_{m,m}^{\mathrm{H}}\boldsymbol{Q}(t_1)\bar{\boldsymbol{h}}_{m,n}\bar{\boldsymbol{h}}_{m,n}^{\mathrm{H}}\boldsymbol{Q}(t_2)\bar{\boldsymbol{h}}_{m,m} \tag{54}$$

$$= \frac{1}{\bar{I}}\frac{\bar{\boldsymbol{h}}_{m,m}^{\mathrm{H}}\boldsymbol{Q}_n(t_1)\bar{\boldsymbol{h}}_{m,n}\bar{\boldsymbol{h}}_{m,n}^{\mathrm{H}}\boldsymbol{Q}_n(t_2)\bar{\boldsymbol{h}}_{m,m}}{\left(1+(t_1/\bar{I})\lambda_n \bar{\boldsymbol{h}}_{m,n}^{\mathrm{H}}\boldsymbol{Q}_n(t_1)\bar{\boldsymbol{h}}_{m,n}\right)\left(1+(t_2/\bar{I})\lambda_n \bar{\boldsymbol{h}}_{m,n}^{\mathrm{H}}\boldsymbol{Q}_n(t_2)\bar{\boldsymbol{h}}_{m,n}\right)} \tag{55}$$

$$= \frac{1}{\bar{I}}\frac{\mathrm{tr}\left(\bar{\boldsymbol{\Phi}}_{m,m}\boldsymbol{Q}_n(t_1)\bar{\boldsymbol{h}}_{m,n}\bar{\boldsymbol{h}}_{m,n}^{\mathrm{H}}\boldsymbol{Q}_n(t_2)\right)}{\left(1+t_1\beta_n(t_1)\right)\left(1+t_2\beta_n(t_2)\right)}, \tag{56}$$

$$= \frac{1}{\bar{I}}\frac{\bar{\boldsymbol{h}}_{m,n}^{\mathrm{H}}\boldsymbol{Q}_n(t_2)}{1+t_2\beta_n(t_2)}\bar{\boldsymbol{\Phi}}_{m,m}\frac{\boldsymbol{Q}_n(t_1)\bar{\boldsymbol{h}}_{m,n}}{1+t_1\beta_n(t_1)}, \tag{57}$$

where

$$\bar{\boldsymbol{\Phi}}_{m,m} = \frac{d_{m,m}}{\sigma_m^2 M_{\lceil m/I\rceil}}\boldsymbol{R}_{m,m},$$
$$\boldsymbol{Q}_n(t) = \left(\frac{t}{\bar{I}}\boldsymbol{H}_{mn}\boldsymbol{H}_{mn}^{\mathrm{H}} + \boldsymbol{I}_M\right)^{-1},$$
$$\boldsymbol{\Delta}(t) = \left(\boldsymbol{I}_{M_{\lceil m/I\rceil}} + \frac{1}{\bar{I}}\sum_{n=1}^{\bar{I}}\lambda_n \bar{\boldsymbol{\Phi}}_{m,n}\frac{t\boldsymbol{I}_{M_{\lceil m/I\rceil}}}{1+t\beta_n(t)}\right)^{-1}, \tag{58}$$
$$\beta_n(t) = \frac{1}{\bar{I}}\mathrm{tr}\left(\lambda_n \bar{\boldsymbol{\Phi}}_{m,n}\boldsymbol{\Delta}(t)\right).$$